THE JOURNAL OF PHYSICAL CHEMISTRY B LETTERS

**2005,** *109,* 18223−18225
Published on Web 09/08/2005



# High-Pressure Neutron Diffraction Study of Superhydrated Natrolite

**Marek Colligan,[†] Yongjae Lee,[‡,§] Thomas Vogt,[‡,||] Aaron J. Celestian,[⊥] John B. Parise,[⊥] William G. Marshall,[#] and Joseph A. Hriljac*[,†]**

*School of Chemistry, The University of Birmingham, Birmingham B15 2TT, U.K., Physics Department, Brookhaven National Laboratory, Upton, New York 11973-5000, Center for Environmental Molecular Sciences and Geosciences Department, State University of New York, Stony Brook, New York 11794, and ISIS Facility, Rutherford Appleton Laboratory, Chilton, Didcot OX11 0QX, Oxon, U.K.*

*Received: July 27, 2005; In Final Form: August 22, 2005*

Neutron powder diffraction data were collected on a sample of natrolite and a 1:1 (v/v) mixture of perdeuterated methanol and water at a pressure of 1.87(11) GPa. The natrolite sample was superhydrated, with a water content double that observed at ambient pressure. All of the water deuterium atoms were located and the nature and extent of the hydrogen bonding elucidated for the first time. This has allowed the calculation of bond valence sums for the water oxygen atoms, and from this, it can be deduced that the key energetic factor leading to loss of the additional water molecule upon pressure release is the poor coordination to sodium cations within the pores.

## Introduction

The response of zeolite structures and properties to applied pressure has been a topic of increasing interest over the past decade.[1−22] One particularly unusual aspect is that the fibrous zeolite natrolite ($Na_{16}Al_{16}Si_{24}O_{80}\cdot 16H_2O$), and several related analogues, undergoes significant unit cell volume expansion under pressure in the presence of a water-containing pressure-transmitting fluid.[1−6] Analysis of synchrotron X-ray powder diffraction data has shown that this is due to the sorption of extra water molecules, pressure-induced hydration (PIH).[1] The PIH of natrolite occurs in stages, resulting in two structural changes.[2] At ∼1.0 GPa, a form of paranatrolite with an ordered distribution of Si and Al atoms is stabilized.[3,4] This contains 24 water molecules per 80 framework oxygen atoms. There is a large volume expansion at the transition (∼7.0%), a reduction in crystallographic symmetry from orthorhombic to monoclinic, and the formation of an additional water bridge between sodium atoms along the elliptical channels. Raman studies show that there is a significant disruption of the hydrogen-bonding network present in the starting natrolite.[2] This was recently confirmed by neutron powder diffraction studies where significant disorder of deuterium positions was found.[4] At ∼1.5 GPa, the system reverts back to orthorhombic symmetry and a superhydrated phase forms with twice the amount of water as that of the starting natrolite, that is, 32 molecules per 80 framework oxygen atoms.[1] Raman studies indicate a reordering of the hydrogen-bonding network formed by the water molecules.[2] Analysis of the X-ray data showed a change in the water network back to a single bridge between the sodium cations, and the oxygen−oxygen distances were suggestive of the possible formation of hydrogen-bonded helical nanotubes of water molecules along the *c*-axis.[1] However, the crystallographic location of the hydrogen atoms in the superhydrated phase has not been determined. We therefore performed a high-pressure neutron powder diffraction experiment to locate the hydrogen atoms and elucidate the details of the hydrogen-bonding network. This allows the first complete description of this system and provides an opportunity to understand all aspects of the reversible nature of the PIH.

## Experimental Section

A powdered crystal (Bound Brook, NJ) was deuterated by vacuum dehydration (70 °C at $1 \times 10^{-4}$ atm and then 200 °C at $\sim 1 \times 10^{-3}$ atm) followed by rehydration with $D_2O$. Deuteration was confirmed by infrared spectroscopy. Neutron diffraction data were collected using the medium-resolution high-flux diffractometer HiPr located on the PEARL beamline of the ISIS Facility at the Rutherford Appleton Laboratory (U.K.). Initially, an ambient pressure pattern was collected with the sample loaded in a sealed 6 mm diameter thin-walled vanadium can. High-pressure diffraction patterns were collected after loading the sample and a small piece of lead into a V3-type Paris-Edinburgh cell equipped with single toroid tungsten carbide (Ni binder) anvils and TiZr capsule gaskets. A perdeuterated 1:1 (v/v) mixture of methanol and water was used as the pressure-transmitting fluid. Short data sets were collected during pressure increase until a clean pattern of the superhydrated phase was obtained. A 10 h data set was collected for analysis at 1.87(11) GPa, as determined from the lattice parameter of lead.

* Corresponding author. E-mail: j.a.hriljac@bham.ac.uk.
[†] The University of Birmingham.
[‡] Brookhaven National Laboratory.
[§] Present address: Department of Earth System Sciences, Yonsei University, Seoul 120749, Korea.
[||] Present address: Nanocenter and Department of Chemistry and Biochemistry, University of South Carolina, Columbia, SC 29208.
[⊥] State University of New York.
[#] Rutherford Appleton Laboratory.

10.1021/jp054142x CCC: $30.25 

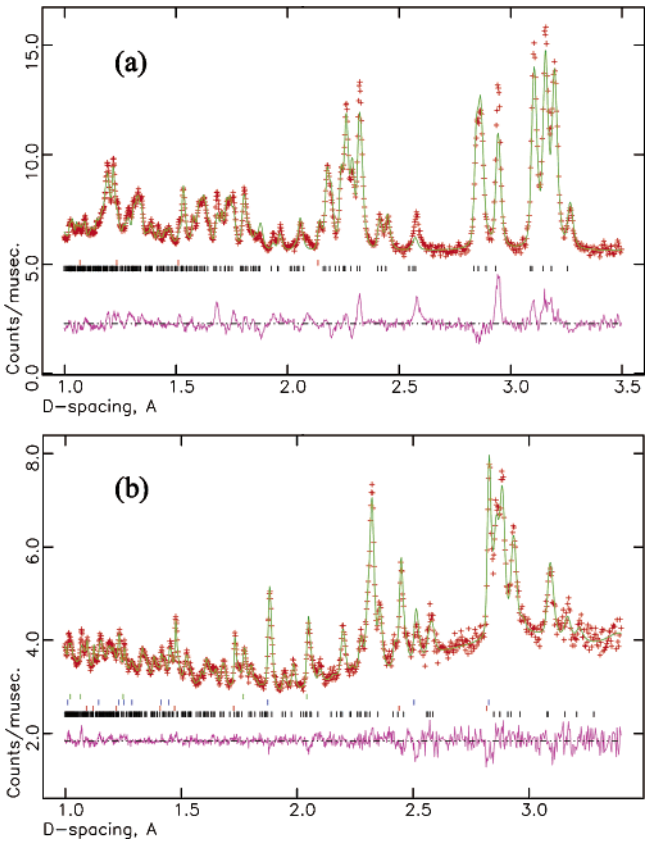


**Figure 1.** Observed (red), calculated (green), and difference (magenta) patterns from the Rietveld analysis of natrolite at (a) ambient pressure and (b) 1.87(11) GPa. The vertical lines indicate the positions of allowed reflections. For part a, these are for natrolite (bottom) and vanadium. For part b, they are for (bottom to top, respectively) natrolite, Pb, WC, and Ni.

Rietveld structure refinements[23] were performed using the GSAS suite of programs.[24] The peak shapes were modeled using TOF profile function 3, a convolution of back-to-back exponentials with a pseudo-Voigt function. For the analysis of the ambient pressure data set, the starting model for natrolite was taken from the literature[25] and vanadium was included as a second phase. For the analysis of the high-pressure pattern, the positions of the non-hydrogen atoms of superhydrated natrolite were taken from the literature[1] and the ATOMS[26] software was used to calculate chemically reasonable starting positions for the four deuterium atoms at distances of 1.00 Å from the water oxygen (Ow) atoms. In addition to the superhydrated phase, lead, tungsten carbide, and nickel were included as additional phases. The positions of all atoms were allowed to vary, with silicon−oxygen, aluminium−oxygen, and oxygen−deuterium bond restraints of 1.62(2), 1.75(2), and 1.00(2) Å, respectively, used to ensure a chemically sound model. For the superhydrated phase, an additional deuterium−deuterium distance restraint of 1.63(2) Å was used to ensure a reasonable D−O−D angle. The restraints could not be removed without introducing some unreasonable distances and angles. Good fits were obtained for both patterns, as shown in Figure 1, with final $\chi^2$ values of 2.226 and 2.416. Complete crystallographic details and tables of distances and angles can be found in the Supporting Information.

## Results and Discussion

The refined model from the ambient pressure data is in excellent agreement with previous work, even though the mineral samples came from different sources.[25] As expected,

**TABLE 1: Selected Distances (Å) and Angles (deg) in Superhydrated Natrolite**[a]

| | Ow−D | D···O | Ow−D···O angle |
|---|---|---|---|
| Ow1−D10···O1 | 0.97(2) | 1.76(3) | 171(3) |
| Ow1−D12···O5 | 0.96(2) | 2.23(3) | 161(3) |
| Ow2−D20···O1 | 1.02(3) | 2.09(4) | 152(3) |
| Ow2−D22···O3 | 0.93(2) | 2.21(4) | 152(3) |
| Ow1−Na | 2.19(7) | D10−Ow1−D12 | 114(3) |
| Ow1−Na* | 2.62(8) | Na−Ow1−Na* | 96(1) |
| | | Na−Ow1−D10 | 117(3) |
| | | Na−Ow1−D12 | 117(4) |
| | | Na*−Ow1−D10 | 93(4) |
| | | Na*−Ow1−D12 | 116(4) |
| Ow2−Na | 2.56(7) | D20−Ow2−D22 | 102(3) |
| | | Na−Ow2−D20 | 110(4) |
| | | Na−Ow2−D22 | 120(4) |

[a] Esd's are in parentheses.

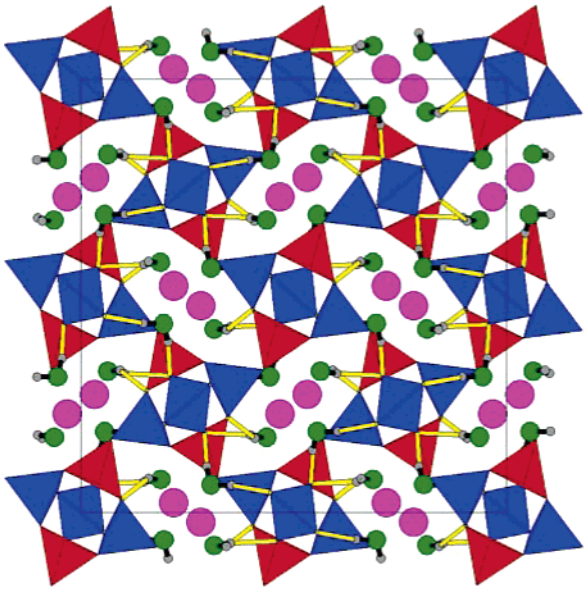

**Figure 2.** Representation of the structure of superhydrated natrolite down (001). Silicon tetrahedra, blue; aluminum tetrahedra, red; sodium atoms, magenta, water oxygen atoms, green; deuterium atoms, gray. Both covalent (black) and hydrogen (yellow) bonds are shown.

the unit cell volume initially decreased with pressure and then dramatically increased with a concomitant change in the complexity of the diffraction pattern as paranatrolite formed.[3,4,27] At 1.44(10) GPa, the pattern could be indexed as monoclinic, space group *Fd*, with a unit cell volume 4.6% larger than that at ambient pressure (2346.5(6) Å$^3$ versus 2243.6(2) Å$^3$).

The analysis of the data collected at 1.87(11) GPa shows the symmetry has changed back to orthorhombic and the unit cell volume decreased to 2267.8(5) Å$^3$. This is still 1.1% larger than that at ambient pressure. The Rietveld analysis of the data confirms that the sample has now become superhydrated[1] and the refined hydration level is 32 molecules per 80 framework oxygen atoms. In this phase, all of the deuterium atoms are ordered and a hydrogen-bonding network including both water molecules forms within the zeolite framework (Table 1, Figures 2 and 3). For the original water molecule, D10−Ow1−D12, a strong hydrogen bond forms from D10 to O1 and a weaker one forms from D12 to O5. This is effectively identical to that previously reported under ambient conditions (H(1)···O(1) = 1.877(2) Å and H(2)···O(5) = 2.103 Å).[25] The water molecule inserted during PIH, D20−Ow2−D22, is also hydrogen bonded to two framework oxygen atoms, but both bonds are weak. Although the distance between water oxygen atoms is only 2.81

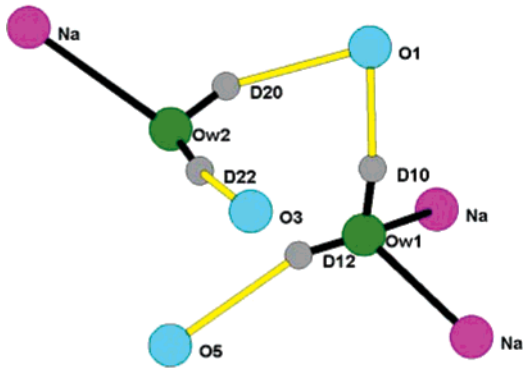


**Figure 3.** View of the bonding of the water molecules, including the localized hydrogen-bonding network.

Å, there is no direct hydrogen bonding, as had been speculated from earlier X-ray diffraction studies. Both water molecules are hydrogen bonded to O1, and this is the only link between them.

The extensive hydrogen bonding in the superhydrated phase raises the question as to why this form is unstable under ambient conditions and dehydrates upon pressure release. We believe the key is the overall bonding of the water molecules within the zeolite (Table 1). Both form two hydrogen bonds to the framework oxygen atoms, but the original water molecule, which remains upon pressure release, is coordinated to two sodium cations, whereas the water molecule introduced under pressure is only coordinated to one sodium cation. The overall bonding energy of the original molecule will be the sum of two strong, coordinate O−Na bonds and two O···D hydrogen bonds, one of which is very strong. The bonding energy of the water molecule introduced by PIH will be much less, as there is only one O−Na bond and two weak O···D hydrogen bonds. Calculations[28] support this: the bond valence sum around Ow1 is 2.09(6), whereas that around Ow2 is 1.72(5). The significant difference is due to the bonding to sodium cations, which contributes 0.46(2) and 0.13(1), respectively. The difference in valence sum contributions from the hydrogen bonding is only 0.11 (0.393(7) for D10···O1 and D12···O5 versus 0.281(5) for D2···O1 and D22···O3). It is therefore principally the weak coordination of the second water molecule to sodium cations that allows it to migrate through the pores and out from the zeolite upon pressure release. We are further investigating the potassium gallosilicate form, which retains the extra water,[5] to see if a similar bonding argument explains the irreversible nature of the PIH in that material.

**Acknowledgment.** This work was supported by a studentship from the EPSRC (M.C.), LDRD from BNL (Pressure in Nanopores), and NSF programs CHE-0221934 and DMR-0452444 (A.J.C. and J.B.P.).

**Supporting Information Available:** CIF files for both refinements. This material is available free of charge via the Internet at http://pubs.acs.org.

## References and Notes

(1) (a) Lee, Y.; Vogt, T.; Hriljac, J. A.; Parise, J. B.; Artioli, G. *J. Am. Chem. Soc.* **2002**, *124*, 5466−5475. (b) Lee, Y.; Hriljac, J. A.; Vogt, T.; Parise, J. B.; Artioli, G. *J. Am. Chem. Soc.* **2001**, *123*, 12732−12733.

(2) Belitsky, I. A.; Fursenko, B. A.; Gabuda, S. P.; Kholdeev, O. V.; Seryotkin, Y. V. *Phys. Chem. Miner.* **1992**, *18*, 497−505.

(3) Lee, Y.; Hriljac, J. A.; Parise, J. B.; Vogt, T. *Am. Mineral.* **2005**, *90*, 252−257.

(4) Seryotkin, Y. V.; Bakakin, V. V.; Fursenko, B. A.; Belitsky, I. A.; Werner, J.; Radaelli, P. G. *Eur. J. Mineral.* **2005**, *17*, 305−314.

(5) Lee, Y.; Vogt, T.; Hriljac, J. A.; Parise, J. B.; Hanson, J. C.; Kim, S. J. *Nature* **2002**, *420*, 485−489.

(6) Lee, Y.; Hriljac, J. A.; Kim, S. J.; Hanson, J. C.; Vogt, T. *J. Am. Chem. Soc.* **2003**, *125*, 6036−6037.

(7) Colligan, M.; Forster, P. M.; Cheetham, A. K.; Lee, Y.; Vogt, T.; Hriljac, J. A. *J. Am. Chem. Soc.* **2004**, *126*, 12015−12022.

(8) Secco, R. A.; Goryainov, S. V.; Huang, Y. *Phys. Status Solidi B* **2005**, *242*, R73−R75.

(9) Arletti, R.; Ferro, O.; Quartieri, S.; Sani, A.; Tabacchi, G.; Vezzalini, G. *Am. Mineral.* **2003**, *88*, 1416−1422.

(10) Havenga, E. A.; Huang, Y.; Secco, R. A. *Mater. Res. Bull.* **2003**, *38*, 381−387.

(11) Comodi, P.; Gatta, G. D.; Zanazzi, P. F. *Eur. J. Mineral.* **2002**, *14*, 567−574.

(12) Ballone, P.; Quartieri, S.; Sani, A.; Vezzalini, G. *Am. Mineral.* **2002**, *87*, 1194−1206.

(13) Ferro, O.; Quartieri, S.; Vezzalini, G.; Fois, E.; Gamba, A.; Tabacchi, G. *Am. Mineral.* **2002**, *87*, 1415−1425.

(14) Moroz, N. K.; Kholopov, E. V.; Belitsky, I. A.; Fursenko, B. A. *Microporous Mesoporous Mater.* **2001**, *42*, 113−119.

(15) Rutter, M. D.; Uchida, T.; Secco, R. A.; Huang, Y.; Wang, J. *J. Phys. Chem. Solids.* **2001**, *62*, 599−605.

(16) Huang, Y.; Havenga, E. A. *Chem. Phys. Lett.* **2001**, *345*, 65−71.

(17) Lui, H.; Secco, R. A.; Huang, Y. *PhysChemComm* **2001**, *8*, 1−3.

(18) Rutter, M. D.; Secco, R. A.; Huang, Y. *Chem. Phys. Lett.* **2000**, *331*, 189−195.

(19) Secco, R. A.; Huang, Y. *J. Phys. Chem. Solids* **1999**, *60*, 999−1002.

(20) Huang, Y. *J. Mater. Chem.* **1998**, *8*, 1067−1071.

(21) Gabuda, S. P.; Kozlova, S. G. *J. Struct. Chem.* **1997**, *38*, 562−569.

(22) Gillet, P.; Malezieux, J.-M.; Itie, J.-P. *Am. Mineral.* **1996**, *81*, 651−657.

(23) Rietveld, H. M. *J. Appl. Crystallogr.* **1969**, *2*, 65−71.

(24) Larson, A. C.; Von Dreele, R. B. *GSAS: General Structure Analysis System*; Report LAUR 86-748; Los Alamos National Laboratory: Los Alamos, New Mexico, 1994.

(25) Artioli, G.; Smith, J. V.; Kvick, A. *Acta Crystallogr., Sect. C* **1984**, *40*, 1658−1662.

(26) *ATOMS*, version 6.1.2; Shape Software: Kingsport, TN, 2004.

(27) Seryotkin, Y. V.; Bakakin, V.; Belitsky, I. A. *Eur. J. Mineral.* **2004**, *16*, 545−550.

(28) Brown, I. D.; Altermatt, D. *Acta Crystallogr., Sect. B* **1985**, *41*, 244−247.